Modeling, Identification and Control, Vol. 46, No. 2, 2025, pp. 51–68, ISSN 1890–1328

A model for the analysis of stomatal dynamics - applied to critical simulations of experiments on oscillatory transpiration in oat plants

T. Brogårdh [1] A. Johnsson [2]

[1] *Corresponding author. E-mail:* torgny.brogardh@gmail.com

[2] *Department of Physics, Norwegian University of Science and Technology, N-7491 Trondheim, Norway.*

Abstract

To explain transpiration results from experiments on stomatal oscillations in oat plants, it is shown by simulations on a model including both hydro-passive and hydro-active feedback that the model must include hydro-active control of the osmotic pressure of the subsidiary cells. Hydro-active feedback was used between the turgor pressure of the mesophyll cells, acting as sensor cells, and the osmotic contents of the subsidiary- and guard cells. In the model, a reduction of the turgor of the sensor cells results in an increase of the osmotic content of the subsidiary cells and a reduction of the osmotic content of the guard cells. Simulations showed that the hydro-active feedback to the subsidiary cells was always needed. However, it was also shown that it is an advantage to combine the hydro-active feedback to the subsidiary cells with hydro-active feedback to the guard cells. The added hydro-active feedback to the guard cells will prevent too high turgor levels in the guard cells when the stomata have closed at water stress with high light levels.

The model consists of established evaporation- and plant waterflow models from literature, experimentally verified models on stomatal mechanics and new models of hydro-active feedback. The model explained results reported in experiments where the water potential of the root medium was lowered and in experiments where the potential rate of evaporation was increased.

Keywords: Stomatal control, hydro-active feedback, oat stomata, grass stomata, plant transpiration control, stomatal oscillations, water stress, modelling, simulation

1. Introduction

The water transpiration of plants occurs through stomatal pores in the leaves. The pore width, which controls the water flux, is regulated by guard cells. Those cells are, however, mechanically affected by neighbors – subsidiary cells and epidermal cells. For details on the stomatal anatomy, see for example Franks and Farquhar (2007).

It is worth noting that the global transpiration through stomata is estimated to account for the cycling of about 60 000 (km)3 water per year, i.e. about $60 \cdot 10^{15}$ kg per year, e.g. Jasechko et al. (2013). This volume is thus transpired in the form of water vapor through plant stomata, whose dimensions are of the order of 10 μm. In this report we will study properties of the plant system controlling this water flux. The model framework and the simulations reveal some hitherto unexplained experimental results.

It has been found, both in natural environmental situations and under experimental conditions, that oscillatory leaf transpiration can take place, Barrs (1971), Hopmans (1971), Cowan (1972), Haefner et al. (1997),

doi:10.4173/mic.2025.2.1

Prytz et al. (2003), Wang et al. (2001) and many others, see e.g. Brogårdh and Johnsson (1973) and Johnsson (2015). Simulations of such oscillations provide crucial tests of dynamic models for plant transpiration control.

Oscillations can be obtained in plant models with hydraulic feedback (also named hydro-passive feedback), where increased volume flow of water through the resistances to water flow in the roots and the leaf, reduces the water potentials of the subsidiary- and guard cells Cowan (1972), Gumowski (1981). In the linear stomatal mechanics model of Cowan, the influence on the stomatal pore opening from the guard cells in relation to that of the subsidiary cells is 1.23, which is higher than the values $0.2 - 0.7$ found in later experimentally obtained non-linear models of the stomatal mechanics of oat Durney et al. (2023) and wheat Franks and Farquhar (2007). Using these non-linear models with lower values of the impact ratio between guard- and subsidiary cells on stomatal pore opening, it was found that stomatal oscillations could not be obtained in simulations using only a hydro-passive model.

The problem to explain experimental results with only hydro-passive control was also pointed out by Buckley (2019). According to Buckley (2019), epidermal- and guard cell turgor pressures decline by similar amounts at an increase in evaporation demand (potential rate of evaporation) in a hydro-passive model. Therefore, stomatal aperture increases and remains elevated instead of obtaining a smaller aperture size as in experiments. Thus, Buckley (2019) concludes that hydro-active control of the stomata is needed. Simulations showing that hydro-active feedback may result in stomatal oscillations and reduced stomatal opening at increased evaporation demand have been demonstrated by Cong et al. (2022, 2024).

Hydro-active feedback (osmoregulation according to Buckley et al. (2003); Buckley (2005) means that plant cells can sense its turgor pressure and respond to lowered turgor pressure by signaling and that this results in changed osmotic content in the guard and/or subsidiary cells. In this context it is well-known that hydro-active feedback is important for the control of the stomatal response to water stress, whereby lowered turgor in cells will activate the synthesis of the plant hormone ABA. This hormone is transported in the plant and will cause stomatal closure to avoid life threatening water loss Kuromori et al. (2018). One question is then if the ABA control is fast enough to be responsible for stomatal oscillations with period times in the region 15 to 40 minutes Johnsson (2015). That this might be the case is supported by the findings of McAdam et al. (2016). They demonstrated rapid synthesis of ABA after application of dry air to leaves. Buckley (2016) found this ABA synthesis to be a possible "black box" that had been opened to explain stomatal response to water status. Later Buckley (2019) writes that there is clear evidence that implicates hydro-active stomatal response including ABA to evaporation demand and soil drought.

The fast ABA synthesis according to McAdam et al. (2016) requires an osmotic response to ABA in the subsidiary cells to explain experimental results with our simulation model. That this could be possible is found in Nieves-Cordones et al. (2022), who have obtained data that AtKC1 (potassium channel α-subunit) can tune the K^+ distribution in the leaf epidermis, leading to increased back pressure of the subsidiary cells at plant water loss. Moreover, Yao et al. 2013 report drought-induced H_2O_2 accumulation in subsidiary cells regulating stomatal aperture of grass plants and Zhang et al. (2020) report increase of H_2O_2 and Ca^{2+} in subsidiary cells during stomatal closure.

The sign of the hydro-active feedback link between the turgor of the sensing cells and the osmotic content of the stomatal cells is important for the dynamics of the system. If the guard cells are the stomatal actuator cells, then the sign must be positive. Using the ABA concept, this means that when the turgor of the sensing cells is reduced, then this will result in outward flow of K^+ from the guard cells (see for example Cotelle and Leonhardt (2019). If, on the contrary, the subsidiary cells are the stomatal actuating cells, then a lowered turgor pressure in the sensing cells must instead give rise to inward flow of K^+ to the subsidiary cells to close the stomata, resulting in negative hydro-active feedback link instead of the positive hydro-active feedback link for the guard cells. This is in accordance with the results of Nieves-Cordones et al. (2022) reporting increased back pressure from the subsidiary cells at plant water loss. It also seems possible from results of Mumm et al. (2011), showing that membrane potential and cytosolic pH determines direction and capacity of ion transport in subsidiary cells. The importance of the subsidiary cells for the stomatal control can also be found in Majore et al. (2002), Büchsenschütz et al. (2005), Wolf et al. (2006) and Liu et al. (2024).

Assuming that fast ABA synthesis is possible for turgor sensing McAdam et al. (2016), the next question is where this sensing takes place. Bauer et al. (2013) and Cotelle and Leonhardt (2019) propose that guard cells have the ABA synthesis themselves, which could mean that guard cells are both the turgor sensing cells and the stomatal actuating cells. McAdam and Brodribb (2018) report that considerable ABA biosynthesis occurred in the mesophyll in water-stressed leaves and point out that ABA synthesis in guard cells cannot easily account for the rapid ABA synthesis caused

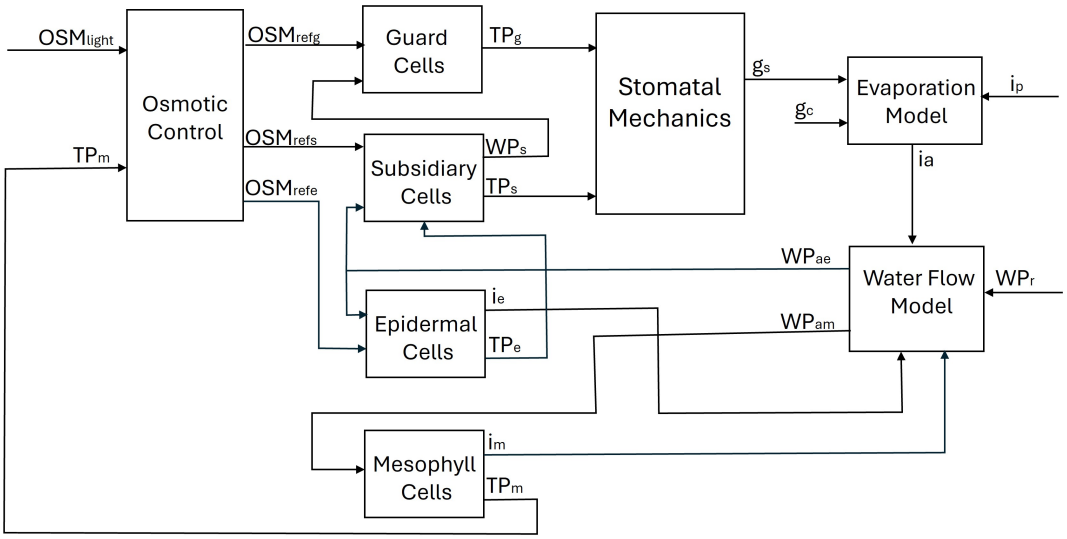

Figure 1: *Overview of the basic model structure used in the simulations. Abbreviations: OSM – quantity of osmotic substance; TP – turgor pressure; WP – water potential; gs – stomatal conductance;* i_p *– potential rate of evaporation;* i_a *- rate of evaporation; i – rate of water flow. Indices: g – guard cell; s – subsidiary cell; e – epidermal cell; m – mesophyll cell; r – root system; c – cuticle; ae – apoplast of epidermis; am – apoplast of mesophyll; ref – reference quantity of osmotic substance; light – light level expressed as resulting quantity of osmotic substance.*

by water-status changes. The results of McAdam and Brodribb (2018) made it a first option for us to use the mesophyll cells as the sensing cells.

2. Overview of the basic model structure

The model structure used in the simulations is shown in Figure 1. The different modules (implemented in Matlab) are described in detail in Appendix A.

2.1. Modules Guard cells, Subsidiary cells, Epidermal cells and Mesophyll cells

The generic implementation of these modules is shown in Figure 5. The hydraulic and osmotic cell dynamics is modelled as a feedback system with the time constant R*C, where R (R_g, R_s, R_e, R_m) is the water flow resistance of the cell wall (in this paper we define cell wall as including the cell membranes) and C (C_g, C_s, C_e, C_m) is the water capacity of the cells. A non-linear relationship is implemented between cell volume and cell turgor (non-linear C) for the guard- and subsidiary cells (see Figure 11). For these cells the osmotic pressure is calculated from the osmotic content and the cell volume, and the osmotic input is the amount of osmotic substance (OSM_{refg}, OSM_{refs}) entering or leaving the cells. Only a simpler model was needed for the epidermal and mesophyll cells, using linear C and osmotic pressure (OSM_{refe}) as input. The water potentials (WP) outside the cells provide the input signals from the hydro-passive feedback. The water potential input to the guard cells can be either WP_s or WP_{ae}. Only results from the first case is presented in this paper. Outputs from the cell modules are turgor pressure (TP) and rate of water flow (i). The rate of water flow was possible to limit whereby, for example, aquaporin effects can be incorporated into the model Cui et al. (2021); Ding et al. (2024). The mesophyll cells are used as turgor (TP_m) sensing cells to adapt to the findings by McAdam and Brodribb (2018). According to results by Nieves-Cordones et al. (2022), water stress will give increased K^+ level throughout the epidermis. To include this effect, the epidermal cells are also arranged to react on TP_m via the osmotic control module. It is assumed that the epidermal cells can cause mechanical pressure TP_e on the subsidiary cells and thus influence the stomatal opening.

2.2. Module Osmotic Control

This module makes hydro-active feedback possible by connecting the turgor (TP) of the sensing cells to osmotic generation in the guard-, subsidiary- and epidermal cells. The implementation of the module is shown

in Figure 6. The hydro-active feedback processes include the generation of hormones in mesophyll cells as response to reduction of turgor (TP_m), the propagation of the hormones to the actuating cells and the receiving and acting on the osmotic content (OSM) of the actuating cells. To make simulations of different cases easier, the hydro-active processes have all been gathered in one module instead of being distributed between different cell types. The output signals OSM_{refg} and OSM_{refs} correspond to quantities of osmotically active substance generated in the guard- and subsidiary cells (K^+ ions pumped in or out through the cell walls). The output signal OSM_{refe} changes the osmotic pressure of the epidermal cells independent of cell volume. The Osmotic Control Module also includes a model of ion flow between the subsidiary- and guard cells, assuming that the subsidiary cells are the K^+ ion storage for the guard cells Raschke and Fellows (1971); Franks and Farquhar (2007). Moreover, an osmotic input OSM_{light} is used to include the light response of the cells. The turgor pressure was selected as the signal between the sensing cells and the Osmotic Control Module since the turgor is the source of strain sensing processes in the cell membranes and the endoplasmic reticulum (Han et al. 2020). The hydro-active feedback links include time constants, delays, one non-linearity and gain parameters. The osmotic control module involves 4 hydro-active negative feedback links. These feedback links result in 4 negative feedback loops for the whole system. Together with the hydro-passive loops, a system of 1 positive and 5 negative interlinked feedback loops is obtained. Systems with such interlinked feedback loops have also been studied in other biological systems Smolen et al. (2001); Cinquin and Demongeot (2002); Tsai et al. (2008).

2.3. Module Stomatal Mechanics

This module relates the stomatal pore opening to the turgor pressures of the guard- and subsidiary cells. The stomatal mechanics models used in the simulations are described in detail in connection to Figures 8 - 10. The inputs to this module are the turgor pressures TP_g and TP_s and optionally TP_e via TP_s. The stomatal pore opening is calculated as pore area (micron^2, Durney et al. (2023) for oat) or as pore width (micron, Franks and Farquhar (2007) for wheat). The stomatal conductance (g_s) is calculated from the stomatal opening values by the multiplication of an opening to conductance constant K_{oc}. in the simulations K_{oc}=0.1 for oat and 1 for wheat. However, using stomata pore opening area as output also from the wheat model, assuming a constant stomata pore length of 10 micron, wheat will also have K_{oc}=0.1.

2.4. Evaporation Module

The evaporation module includes the conductance of the cuticle (g_c), a boundary layer parameter (h) and the potential rate of evaporation (i_p). The leaf conductance (g_l) is obtained as (g_c + g_s), where g_s is the stomatal conductance. The module (see Figure 7A) is implemented according to the evaporation model of Cowan (1972).

2.5. Water Flow Module

The water flow module (implementation shown in Figure 7B is based on the resistor network in "Plant Water Relations" in Figure 3 of Cowan (1972). It includes the resistances to water flow through the root system and the leaf and calculates the water potentials in the apoplasts of the mesophyll (WP_{am}) and epidermis (WP_{ae}). To calculate WP_{am} and WP_{ae}, the waterflow currents i_a, i_m, i_e, i_s and i_g are used (i_s and i_g connections not shown in Figure 1. The water flow model also includes the water potential of the root medium (WP_r).

It should be mentioned that variables and parameters are scaled according to Cowan (1972) to represent averages per unit area of a leaf. For example, cell water flow speed of 10^{-4} mm/s in the model corresponds to the water flow speed 10^{-3} mm^3/s if the leaf area is 10 mm^2.

3. Changing Water potential of root medium

To test the model on critical dynamic cases, we have simulated experiments on lowering the water potential (WP_r in Figure 1) of the medium surrounding the roots of an oscillating oat plant, Brogårdh et al. (1974). The experiments resulted in lowered rate of transpiration and in one case (Figure 1C in their publication) in damping of the oscillations (when lowering the root water potential to -3.2 bar). The oscillations stopped when the root water potential was reduced to -5 bar.

To test our model approach, we simulated these experiments by using the model structure in Figure 1 with the modules described in Appendix A. At first the oat stomatal mechanics model according to Figure 9 was implemented and then the wheat stomatal mechanics according to Figure 10B. The hydro-passive feedback parameters were based on the parameters used by Cowan (1972) and the hydro-active parameters (in Figure 6) were tuned to obtain oscillations. All parameters used in the simulations are listed in Appendix B.

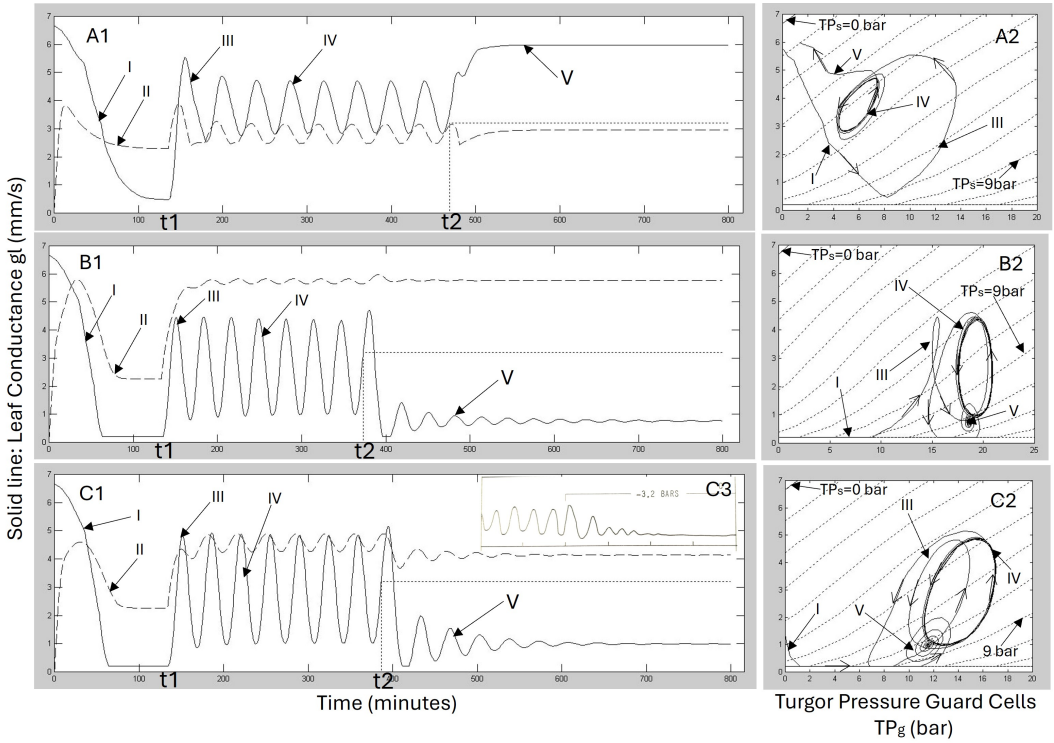

Figure 2: *Simulation results for stomatal oscillations using the oat stomatal mechanics according to Figure 9. Solid lines represent leaf conductance g_l (mm/s) and broken lines osmotic pressure of guard cells (multiplied by 0.25 to use the same y-axis scale, 0.25·OP_g bar). The dotted lines in the left figures represent the water potential of root medium (with reversed sign, -WP_r bar). The left figures show how the variables change with time and the right figures with respect to the turgor pressures of the guard cells (TP_g) and the subsidiary cells (TP_s). The dotted lines in the right figures are obtained at constant TP_s-values and the difference in TP_s between 2 dotted lines is 1 bar (see Figures 8 - 9). The propagation directions of the trajectories are indicated by arrows. The inserted Figure C3 is taken from experimental recordings.*

3.1. Hydro-active feedback with oat stomatal mechanics

To replicate the experiments of Figure 1C in Brogårdh et al. (1974), simulations were made in three cases. In the first case hydro-active feedback was made only to the guard cells (2A1 and 2A2-figures), in the second case only to the subsidiary cells (2B1 and 2B2-figures) and in the third case both to the guard- and subsidiary cells (2C1 and 2C2-figures). All default parameter values as well as simulation specific parameter values can be found in Appendix B. At the start of the simulations (time 0), the filling of the cells with osmotic active substance (OSM_{tp0g}, OSM_{tp0s} and OSM_{tp0e}, Figure 6) starts to obtain correct turgor pressure in darkness at WP=0 (TP_{0g}=9 bar, TP_{0s}=9 bar). The application of OSM_{tp0} results in transients I and II. At t_1 light is applied (the output of SF in Figure 6 is set to 1) and oscillations (IV) are achieved. At t_2 the root water potential (WP_r, Figure 7B) is lowered from 0 to -3.2 bar as in the experiments.

In Figure 2A1 the leaf conductance g_l increases to a constant high level after the reduction of WP_r at t_2, but in 2B1 and 2C1 g_l is reduced and damped oscillations are achieved as in the experiments (inserted Figure 2C3, which is a copy of Figure 1C in Brogårdh et al. (1974). The result in Figure 2A1 is thus not correct in relation to the experimental results. Moreover, it seems to be a bad strategy for the plant to increase the leaf water conductance at water stress. What should also be observed is the oscillation amplitude of the osmotic pressure (OP_g) of the guard cells (broken line, 0.25·OPg). In relation to the oscillation amplitude of leaf conductance (g_l, solid line), the OP_g-ocillations are larger in Figure 2A1 than in 2C1, which is larger than in 2B1. Wang et al. (2001) showed that the K^+ concentration in guard cells of Glycyrrhiza plants did not oscillate during stomatal oscillations. If these results can be transferred to oat stomata, it will further

reduce the likelihood for oscillations with hydro-active feedback only to the guard cells according to Figure 2A1.

Now, comparing Figure 2A2 with 2B2 and 2C2, it is evident that the oscillations (IV) and the WP_r-response (V) take place at much lower turgor pressures (TP_g, TP_s) in Figure 2A2 than in 2B2 and 2C2. The results in Figure 2A2 after lowering WP_r should be a bad strategy with low turgor pressure levels (approaching plasmolysis) of the guard- and subsidiary cells. Furthermore, comparing Figure 2B2 with 2C2, it could be argued that the higher level of especially TP_g but also TP_s in Figure 2B2 at water stress could be a disadvantage. What happens is that the turgor pressure TP_s of the subsidiary cells must be high enough to reduce the stomatal opening when the turgor pressure TP_g of the guard cells is high because of the light level (OSM_{light}, see Figure 6). The added hydro-active feedback to the guard cells will reduce TP_g and consequently the level of TP_s needed to close the stomata will also be reduced.

Summing up, it seems evident from the simulation results with the stomatal mechanics model for oat plants, based on Durney et al. (2023), that hydro-active feedback to the subsidiary cells is needed and it is not possible to reproduce the experiments with hydro-active feedback to only the guard cells. However, even if the former experimental results cannot verify it, the simulations show that a combination of hydro-active feedback to both the subsidiary- and guard cells seems to be the most efficient and probable arrangement for stomatal control.

It should be mentioned that it is not possible to obtain oscillations in the simulations using only hydro-passive feedback. This is because the influence of TP_s on stomatal opening is too high in relation to TP_g when using the stomatal mechanics model of oat (and also wheat). To reduce the influence of TP_s, the value of OSM_{tp0s} (see Figure 6) can be increased. When this is made, such that TP_{0s} is increased from 9 bar to 15 bar, oscillations can occur. The response to lowered WP_r is, however, then the same as the response at hydro-active feedback to only the guard cells and cannot explain the experimental results.

3.2. Hydro-active feedback with wheat stomatal mechanics

Figure 3 shows results of simulations made with the wheat stomatal mechanics model, Franks and Farquhar (2007) according to Figure 10B. As in Figure 2, Figure 3A is obtained with hydro-active feedback only to the guard cells, Figure 3B only to the subsidiary cells and Figure 3C both to the guard-and subsidiary cells. At the start of the simulations (time 0), the cells are filled with osmotic active substances (OSM_{tp0} applied, see Figure 6), which results in transients I and II. At t_1 light is applied and oscillations (IV) are obtained. At t_2 the root water potential (WP_r) is lowered from 0 to -3.2 bar and as can be seen, the level of leaf conductance g_l is reduced in all cases. To differentiate between the cases, WP_r is further reduced from -3.2 to -5 bar (at time t_3). The level of g_l is then further reduced in Figures 3B1 and 3C1 but increased in 3A1. Therefore, it seems that the response in 3A1 after t_3 (when WP_r is further reduced) is not correct. Increasing water stress should close the stomata further. Unfortunately, this cannot be proved by the experimental recordings in Figure 1D in Brogårdh et al. (1974), where the levels of transpiration rates after lowered root water potential could not be compared between Figures 1C for -3.2 bar and 1D for -5 bar.

As in Figure 2, the oscillation amplitude of the osmotic pressure (OP_g) of the guard cells (broken line, $0.25 \cdot OP_g$) in relation to the oscillation amplitude of leaf conductance (g_l, solid line) is larger in 3A1 than in 3C1, which in turn is larger than in 3B1. As for the simulations of the oat model in Figure 2, this makes it difficult to explain the results of Wang et al. (2001) with only feedback to the guard cells according to Figure 3A1.

Comparing Figure 3A2 with 3B2 and 3C2, it is evident that the oscillations (IV) and the response (V, VI) to lowered root water potential (WP_r) take place at lower turgor pressures (TP_g and especially TP_s) in 3A2 than in 3B2 and 3C2. As in the oat-case, it seems to be a bad strategy with only hydro-active feedback to the guard cells resulting in very low turgor TP_s of the subsidiary cells at water stress. Looking at the results in Figure 3B2, it is evident that the trajectories IV, V, VI reach even higher values of the turgor of the guard cells TP_g than in the oat case (Figure 2B2). This depends mainly on the higher light level used in the simulations of Figure 3 than in Figure 2.

Summing up, it seems evident also from the simulation results with the stomatal mechanics model for wheat, based on Franks and Farquhar (2007), that hydro-active feedback to the subsidiary cells is necessary. To avoid too high turgor TP_g of the guard cells, it is also advantageous for wheat plants to use a combination of hydro-active feedback to both the guard- and subsidiary cells as in Figure 3C.

With respect to hydro-passive oscillations (obtained with higher value of TP_{tp0s}), the response to lowered WP_r was found to be the same for wheat as for oat.

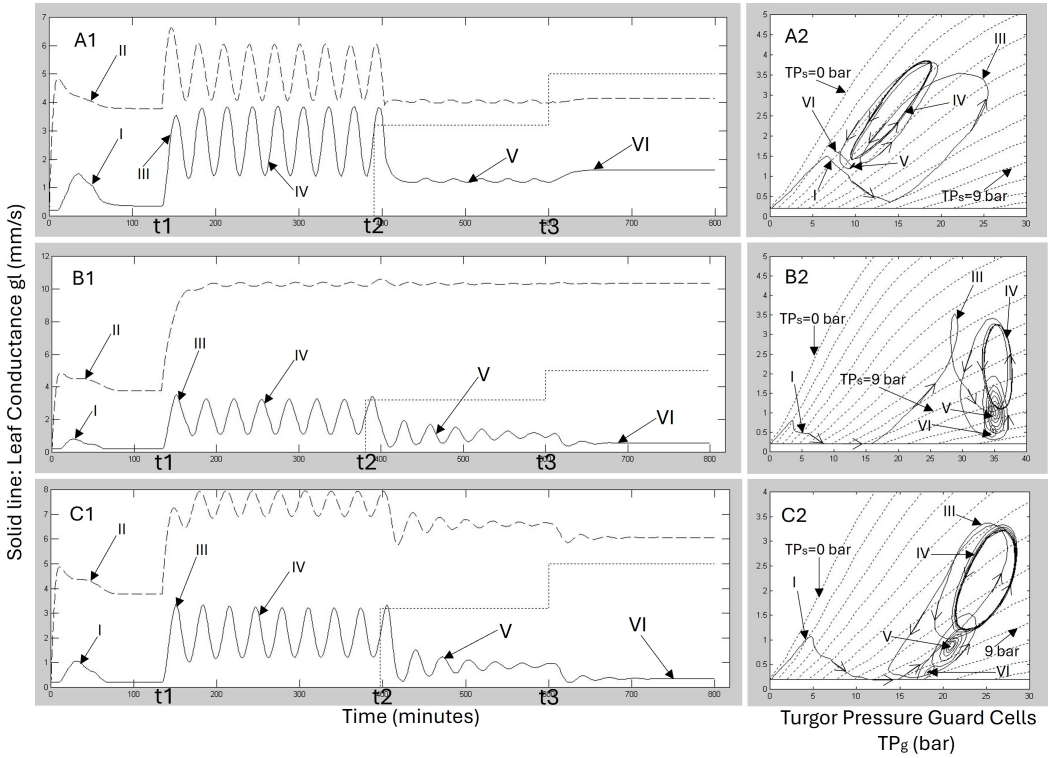

Figure 3: *Simulation results for stomatal oscillations using the wheat stomatal mechanics according to Figure 10B. Solid lines leaf conductance g_l (mm/s), broken lines osmotic pressure of guard cells plotted as 0.25·OP_g (bar), dotted lines in left figures water potential of root medium with reversed sign, -WP_r (bar). The left figures show how the variables change with time and the right figures with respect to the turgor pressures of the guard cells (TP_g) and the subsidiary cells (TP_s, dotted lines). The dotted lines are obtained at constant TP_s-values and the difference in TP_s between 2 dotted lines is 1 bar. The propagation directions of the trajectories are indicated by arrows.*

4. Changing Potential Rate of Evaporation i_p

Another critical test, using experimental results in literature, is about the stomatal response to increasing potential rate of evaporation i_p, obtained by lowered air humidity and/or increasing wind speed. Increased ip should at first give a transient with increased stomatal opening, named WWR, Wrong Way Response. Then a reduction of the stomatal opening should take place until it reaches a level, lower than the one before the increase in ip (Figure 3 in Buckley (2019). Experimental results showing that the steady state stomatal pore width is lower when i_p is higher can also be found in Figure 5 of Franks (2004) and in Figure 9 of Franks and Farquhar (2007).

In Figure 4 the cells are at first (time 0) provided with osmotic substance (OSM_{tp0}) to obtain the turgor levels (TP_0) at darkness and WP=0. The responses to these actions (I) end up with closed stomata (g_l=g_c, Figure 7A), TP_{0g}=9 bar in oat (Figure 4A2), TP_{0g}=15 bar in wheat (Figure 4B2) and TP_{0s}=9 bar in both oat and wheat. At time t_1 (Figures 4A1 and 4B1), light is applied at potential rate of evaporation i_p=0 mm/s. The response to light (II) ends up with a constant level of leaf conductance g_l (III). At time t_2 the potential rate of evaporation (i_p) is increased and after a transient (WWR IV), new levels of leaf conductance (V, VI, VII) are obtained. Level V is reached when using only hydro-active feedback to the guard cells, VI only hydro-active feedback to the subsidiary cells and VII with combination of hydro-active feedback to both the guard-and subsidiary cells. When combined (VII), the same hydro-active feedback gains (K_g, K_s) are used as in the individual cases (V and VI). In both the oat- and wheat cases, it is evident that the combined hydro-active feedback (case VII) is most efficient with respect to lowering the leaf conductance. Moreover, the combined feedback also results in the highest TP_s-level after increasing i_p (case VII in Figures 4A2 and 4B2). Thus, the best strategy should be combined hydro-active feedback.

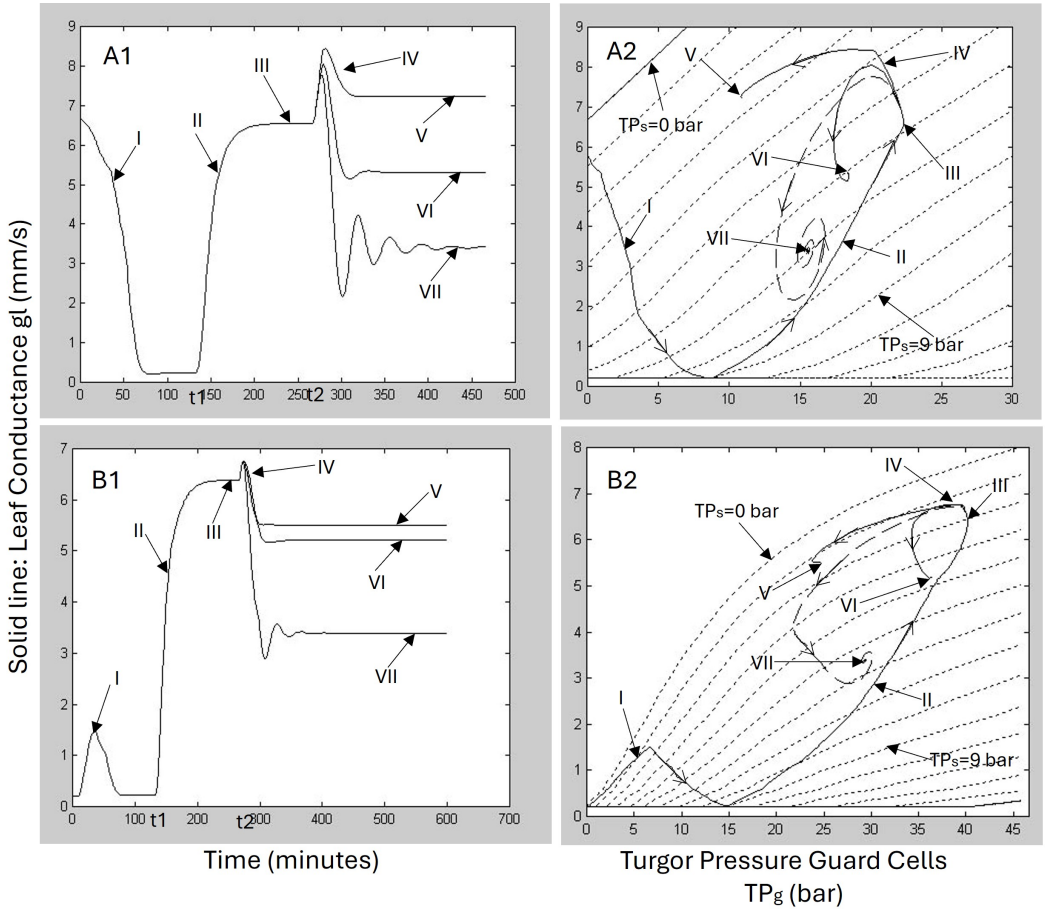

Figure 4: *Simulation results of sudden increase of potential rate of evaporation ip with oat stomata (A) and with wheat stomata (B). The leaf conductance g_l (mm/s) is shown as a function of time in A1 and B1 and as function of the turgor of guard- and subsidiary cells in A2 and B2. Dotted lines in A2 and B2 show turgor of subsidiary cells (TP_s).*

Figure 4 also shows that there are damped oscillations in the responses to the increased potential rate of evaporation i_p in the combined case (VII). Lowering i_p further will start sustained oscillations. Oscillations as response to increasing evaporation demand has also been seen experimentally, see Figure 1 of Farquhar and Cowan (1974).

5. Conclusions

The conclusions that can be drawn from the modelling and simulations of critical tests in this paper:

- Based on references in literature, a model could be built to verify published experimental results. In the model, the mesophyll cells were used as turgor pressure sensing cells, producing a hormone (ABA?) signal as response to water stress. This was modelled using a threshold turgor level, under which the formation of the hormone takes place, and a time constant for the hormone generation process. Time delays were then implemented for the transport times of the hormone together with time constants for the formation of osmotic substance (K^+ ions?) in the subsidiary- and guard cells. Adopting this model interlinked with a hydro-passive model based on a model of Cowan (1972), it was possible to explain experiments on stomatal oscillations when the water potential of the root medium was lowered. It was also possible to explain why the stomatal opening is reduced when the potential rate of evaporation is increased.

- The model simulations showed that when the control of oat- and wheat stomata consists of one positive and one negative hydro-passive feedback loop and one or more interlinked hydro-active feedback

loops, then one of the hydro-active feedback loops must involve the subsidiary cells, otherwise it is not possible to obtain the same results as in experiments.

- The model simulations also showed that if only hydro-active feedback is applied to the guard cells, the turgor pressure of the subsidiary cells will be very low at low water potential of the root system. On the other hand, if only hydro-active feedback is applied to the subsidiary cells, the turgor pressure of the guard cells will be very high at high light levels and at low water potential of the root system. The simulations moreover showed that these two problems can be solved by using hydro-active feedback to both the guard-and subsidiary cells.

6. Future Work

Based on the models presented in this paper, further model studies and simulations will be performed.

One possibility is to extend and adapt the model to other existing, and new, experimental results. These may include the influence on stomatal control of for example light levels, blue/red light, CO_2-levels, temperature, leaf water flow resistance, chemical treatments and genetic modifications.

Future work could also include studies of hydro-passive and hydro-active couplings between different segments of a leaf, coupled oscillators, forced oscillations, singularities and phase relations.

It would also be interesting to find out if the model can be used to simulate oscillations in other than grass plants. Then stomatal mechanics models, according to for example Figure 6 in Franks and Farquhar (2007), are needed for plants in which stomata can oscillate without having subsidiary cells (as for example in cotton).

To reduce the parameter sensitivity, the model may need more non-linearities together with speed limiting and damping components. This will target different processes in the involved cell types, as for example the aquaporin control and the processes involved in hydro-active feedback.

Hopefully, accurate modelling of stomatal control can be a tool to predict and optimize genetic engineering for improved water stress resilience in plants.

A. Description of the modules in Figure 1

A.1. The cell module

The cell model calculates water flow speed i (mm/s) through the cell wall, the cell volume changes dw (mm), the complete cell volume W (W_0 + dw mm, where W_0 is the cell volume at TP=0 bar), the turgor pressure TP (bar), the internal water potential WPint (bar) and the osmotic pressure OP (bar). To make these calculations, the following inputs are used: the external water potential WPext (bar), external pressure on the cell wall TPext (bar) and the amount of osmotic substance OSMref (scaled to result in bar·mm after multiplication with $5 \cdot 10^5$) passing the cell wall (including the cell membrane). The internal water potential of the cell WPint (bar) is used for feedback and is connected to the input WPintin. The cell volume outputs dw and W are used for tuning purposes. Model parameters are the cell wall resistance to water flow R (bar · s/m), the water capacity of the cell C (m/bar), the cell volume W0 (mm) at turgor pressure TP=0 bar and the ratio Kxy of TPext performing back pressure on the cell (only Kes has been studied). Parameters in triangles are scaling factors to adapt to the scaling used in the paper of Cowan (1972). When switch S is in position s1, the OSMref-values (bar·mm·$5{\cdot}10^5$) are used as scaled osmotic content passing the cell wall. The scaling corresponds to a value of n*R*T, where n is the number of moles, R the ideal gas constant and T the temperature in Kelvin. It is assumed that experiments were done at constant temperature. In position s2 the OSMref input (bar) is directly used as the osmotic pressure of the cell. Position 2 was used for epidermal- and mesophyll cells. Tests were made in position 1 also for these cells. The same results were possible to obtain but the solver had sometimes problems with this configuration. The module 1/X inverts the input signal and 1/s accomplishes integration, where s is the Laplace variable. NL_{dw} is introduced to obtain non-linear relationship between the turgor pressure of the cells (TP) and the volume changes (dw) as reported by Franks et al. (2001), see Figure A7. The module N_{Li} is used to limit the water flow through the cell walls. This simulates possible aquaporin effects. At present only fixed limits are used, but simulations could be made with N_{Li}-limits dependent on the turgor pressure of the cells Cui et al. (2021); Ding et al. (2024).

A.2. The osmotic control module

The osmotic inputs to the osmotic control module are the turgor pressure of the mesophyll cells TP_m (bar) and the light level OSM_{light} (scaled as bar·mm·$5{\cdot}10^5$).

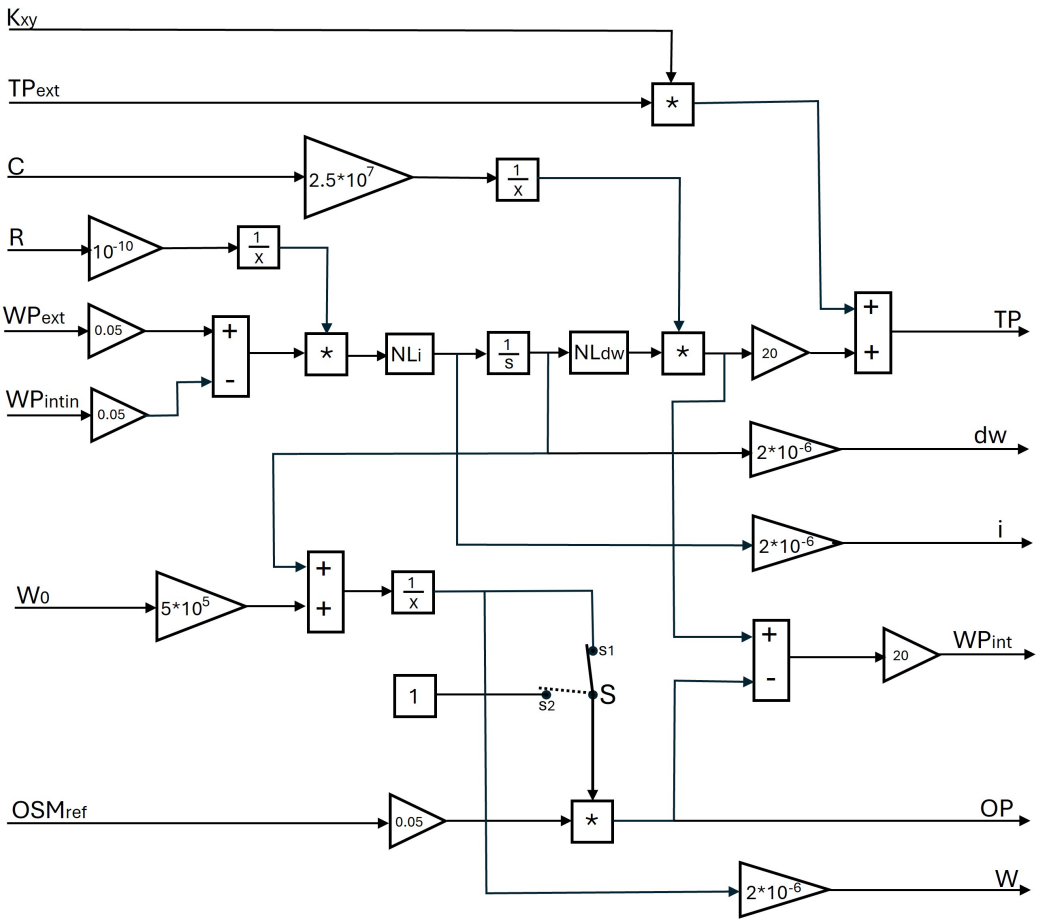

Figure 5: *The generic module for cells describes the dynamical properties of the cells with respect to its content of water and osmotic substances.*

Output signals are the amount of osmotic substance OSM_{refg}, OSM_{refs} (bar·mm·5·10^5). To facilitate the simulations, OSM_{refe} is instead defined as osmotic cell pressure (bar). Several design parameters are included. $TP0_m$ (bar) is the turgor of the mesophyll cells at WP_{intm}=0 bar (see Figure 5). OSM_{tp0g} and OSM_{tp0s} (bar·mm·5·10^5) are the amounts of osmotic substance applied to the guard- and subsidiary cells at the start of the simulations to obtain full cell turgor levels (TP_{0g} 9 bar for oat and 15 bar for wheat and of TP_{0s} 9 bar for both oat and wheat). OSM_{tp0e} (here defined in bar) is the osmotic pressure (resulting in TP_{tp0e} = 9 bar) for the epidermal cells to obtain full turgor. The turgor pressures TP_0 for the cells are built up before OSM_{light} is applied. TP_0 is defined for full turgor according to Figure 4 of Franks et al. (1998). The nonlinearity NL with the input (TP_m-TP_{0m}) determines that only values of TP_m-TP_{0m} below TP_{thr} (bar) will result in hydro-active feedback. The hydro-active feedback loop from the mesophyll cells contains time constant T_{sensm} for the sensing process in the mesophyll cells. An added lower limit could also be used to limit the ABA synthesis. A delay time $dt_{transpe}$ is defined for hormone (ABA) transport from the mesophyll cells to the epidermal cells and a corresponding delay time $dt_{transps}$ is defined for hormone transport to the subsidiary cells. It is assumed that the hormone transport to the guard cells passes via the subsidiary cells and the delay time from the subsidiary cells to the guard cells is defined as $dt_{transpg}$. In each type of actuating cells there is a time constant (T_{actg}, T_{acts}, T_{acte}) for the actuation processes. Each hydro-active loop has a gain (K_e, K_s, K_g). The gain K_{gs} is used to calculate the influence of OSM_{refg} (OSM_{tp0g} excluded) on OSM_{refs} using the approach that the subsidiary cells are the K^+ ion pool for the guard cells Raschke and Fellows (1971); Franks and Farquhar (2007). Nonlinear relationships between turgor pressures and cell volumes for the guard-and subsidiary cells were designed (parameters NL_g, C_g, W_{0g}, NL_s, C_s and W_{0s}, see Figure 11 to obtain expected response to OSM_{light} at K_{gs} = -1, meaning that all ions added to the guard cells originate from the subsidiary

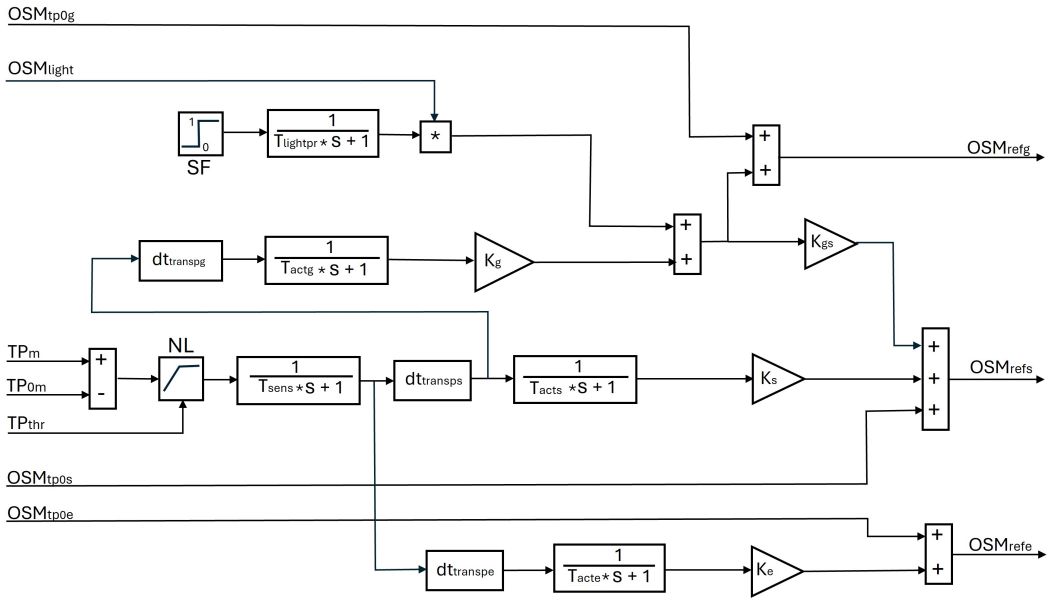

Figure 6: *The osmotic control module gathers processes for turgor pressure sensing in mesophyll cells, hormone transmissions in the leaf and osmotic action in the guard, subsidiary and epidermal cells. Moreover, it also contains the osmotic light response in the guard cells and the osmotic substance transport between the guard-and subsidiary cells.*

cells. A light step is obtained from the step function SF (step from the value 0 to 1) via a time constant ($T_{lightpr}$) for the light induced processes and a multiplication with the selected light level OSM_{light}, which is scaled as bar·mm·5·10^5. All time constants scaled according to Cowan (1972), resulting in time constant values in minutes after multiplying with scaling factor 6.67. In the presented simulations the mesophyll cells were used as sensing cells based on McAdam and Brodribb (2018). It should be mentioned that the reason for using TP_m -TP_{0m} as input and not the water potential (WP_m) is that changes in WP_m will not correspond to changes of TP_m-TP_{0m} when water capacities of the cells are non-linear and/or when the osmotic pressure changes during the simulations. The modelled hydro-active feedback links will add 4 negative feedback loops with gains K_g, K_{gs}, K_s and K_e to the hydro-passive feedback loops (one positive and one negative). These 6 loops are interlinked Cinquin and Demongeot (2002); Tsai et al. (2008) and the control properties of the system are of importance. A preliminary study shows that using only the hydro-passive feedback loops (at lower influence on the stomata opening from the guard cells than from the subsidiary cells), the system will be unstable without oscillations at increased common loop gain. This depends on a phase shift for the open system of 180 degrees at low frequencies. When increasing the common feedback gain to get zero amplitude margin, the system states will immediately obtain large values, and no oscillations can be obtained. Introducing the hydro-active feedback links with the gains K_s and K_g, stable oscillations with a specific frequency will instead appear. The feedback link to the subsidiary cells with gain K_s works as an efficient phase compensating filter advancing the phase of the hydro-passive system at low frequencies from 180 degrees to zero degrees. In this way, the only frequency, for which the system can be unstable, is the oscillation frequency. The feedback link to the guard cells with gain K_g acts as an added low pass filter and will not change the phase of 180 degrees at lower frequencies. However, it will reduce the gain at lower frequencies in relation to the gain at an oscillation frequency (also with 180 degrees phase shift). In this way the amplitude margin will be higher at low frequencies than at the oscillation frequency and the feedback to the guard cells can perform oscillations before it gets unstable at low frequencies.

A.3. The evaporation and water flow modules

The input signal to the evaporation module, Figure 7A, is the stomatal conductance g_g (mm/s) and the output signal is the rate of evaporation i_a (mm/s). Parameters used to modify the evaporation demand are the conductance of the cuticle g_c (mm/s), the potential rate of evaporation i_p (mm/s) and the heat/vapor conductance of the leaf boundary layer h (mm/s).

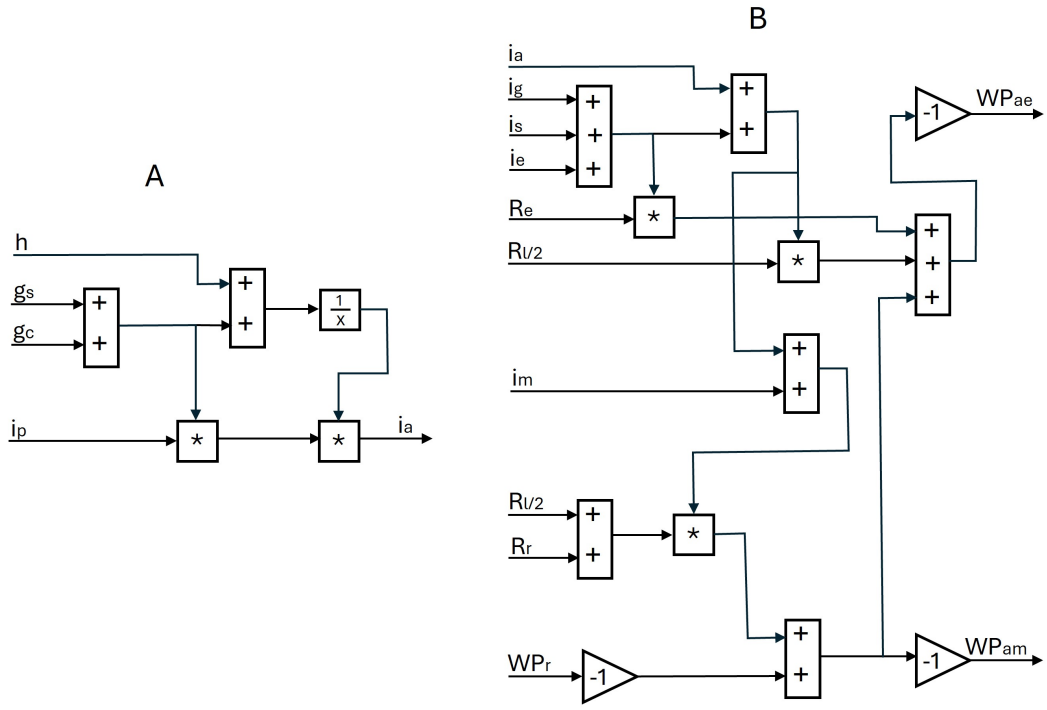

Figure 7: *A: The evaporation module, which is the same as used by Cowan (1972). B: The water flow module based on Cowan (1972).*

Input signals to the water flow module, Figure 7B, are the rate of evaporation i_a, the rates of waterflow i (mm/s) through the cell walls of the different cell types (i_m for mesophyll cells, i_e for epidermal cells, i_s for subsidiary cells and i_g for guard cells) and WP_r (bar), the water potential of the root medium. Output signals are the water potentials (bar) of the apoplast of the mesophyll WP_{am} and of the apoplast of the epidermis WP_{ae}. Resistance components R for waterflow (bar·s/m) are arranged according to Cowan (1972) with R_r as the root resistance, $R_l/2$ as half of the leaf resistance and R_e as the resistance in the epidermis. It is assumed that i_m will contribute to the water flow through $R_r+R_l/2$. More studies are needed to understand how flows of water in and out of different cell types influence the water potential in different parts of the leaf. However, this was not found critical for the results of this paper.

A.4. The stomatal mechanics module for oat plants

The stomatal mechanics model describes how the stomatal pore opening (in micron or micron^2) depends on the turgor of the guard- and subsidiary cells. This is a non-linear model of great importance for the control of stomatal opening. The models used in this paper originate from two publications Durney et al. (2023) for oat and Franks and Farquhar (2007) for wheat) and were implemented as piecewise linear functions.

Figure 8A shows a reconstructed version of the oat model in Figure 2A of Durney et al. (2023). The turgor pressure TP_s of the subsidiary cells is constant for curves I and II and for the interpolated curves in between (as curve III). Therefore, we will further on name these curves TP_s-curves. For the upper TP_s-curve I, TP_s= 2 bar and for II, TP_s= 7 bar. The dotted TP_s-curves (III) are obtained with equidistant (1 bar) constant values of TP_s between 2 and 7 bar.

Curve IV shows how TP_g may influence TP_s when the guard- and subsidiary cells are osmotically connected. As can be seen, curve IV does not follow the TP_s-curve II for TP_s=7 bar. This is because OSM_{refs} decreases when OSM_{refg} increases (parameter K_{gs} in Figure 6). In Figure 8B the ranges of TP_s and TP_g were extended to the ranges that Franks and Farquhar (2007) used in their measurements of stomatal mechanics for wheat. Thus, the lowest value of TP_g is now 0 bar and full subsidiary cells turgor TP_{0s} is set to 9 bar, Figure 4 of Franks et al. (1998). TP_{0s} is obtained when WP_{ints}=0 bar, Figure 5, in darkness.

TP_s-curve parts I and II (solid lines) in Figure 8B are the same as in Figure 8A with TP_s = 2 and 7 bar. TP_s-curve III is for 5 bar, V with TP_s = TP_{0s} = 9 bar and VI with TP_s=0 bar. TP_{0g} (9 bar) is obtained

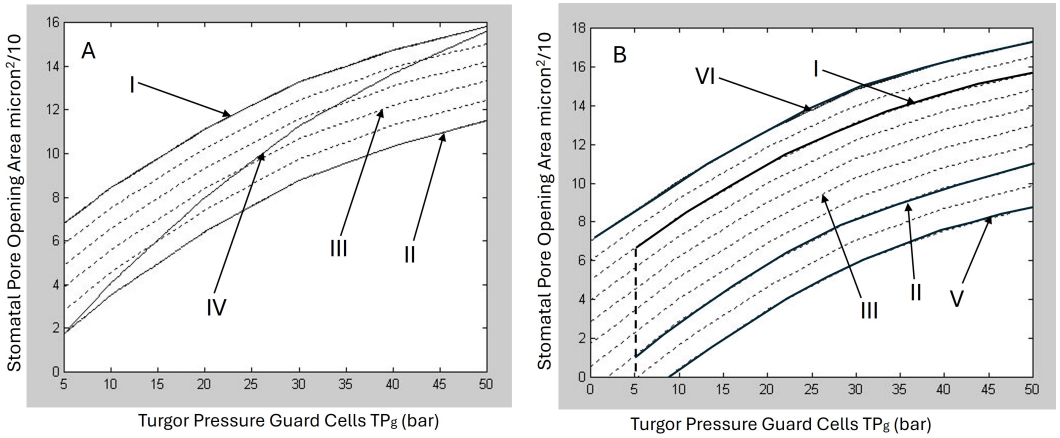

Figure 8: *The Stomatal pore area as function of the turgor pressure (TP_g) of the guard cells at different values of the turgor pressure TP_s of the subsidiary cells (shown by broken and full drawn curves; I – IV). A: Model for oat, based on Figure 2A in Durney et al. (2023). B: An extension according to Franks and Farquhar (2007) of the model in figure A.*

when stomatal pore opening is zero at full subsidiary cells turgor TP_{0s}.

Looking at figures 1, 4 and 5 of the work of Franks et al. (1998), it is obvious that the derivative of TP_s-curves is reduced when the stomatal opening width approaches zero. This effect can also be discerned at TP_s=7 bar in Figure 2A of Durney et al. (2023). To introduce this effect in the stomatal mechanics model of Figure 8B, an additional nonlinearity was introduced. Figure 9 shows the model when this was made, reducing the slopes at smaller stomatal openings of the TP_s-curves. TP_s-curves (broken lines) for TP_s-values higher than TP_{0s} (9 bar) have also been introduced in Figure 9 (for example VII for 10 bar). The reason for this is that hydro-active feedback to the subsidiary cells may give higher TP_s-values than full cell turgor TP_{0s}.

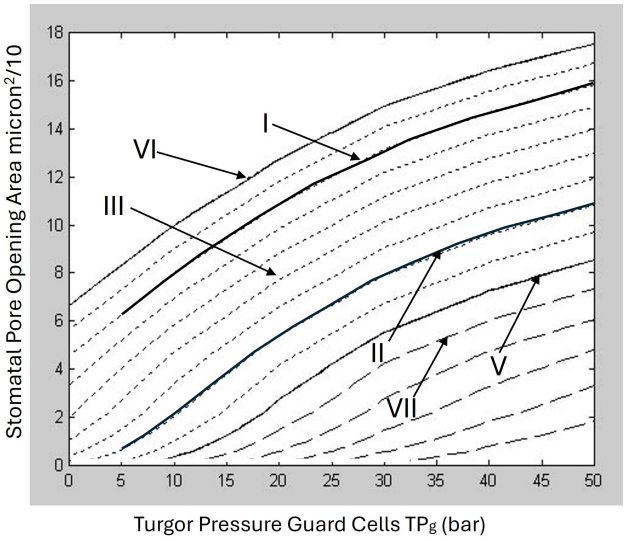

Figure 9: *An additional nonlinearity was introduced into the model of Figure 8B to reduce the derivative of the TP_s-curves at lower values of the stomatal opening.*

A.5. The stomatal mechanics module for wheat plants

To achieve an experimentally verified stomatal mechanics model for wheat, Figure 6D in Franks and Farquhar (2007) was used as a starting point. This figure shows experimental data for stomatal opening vs guard cells turgor in the cases of zero epidermal turgor and full epidermal turgor. In this paper we assume that the subsidiary cells turgor equals the measured epidermal turgor. The value of full turgor TP_{0s} of the epidermis was reported to be 9.2 bar, Franks et al. (1998). To have numerically simpler equidistant TP_s-curves (from 0 bar), TP_{0s} is set to 9 bar. This wheat model has earlier been used in stomatal simulations, Cong et al. (2022).

Looking at Figure 10A, TP_s = 0 bar for TP_s-curve I and TP_s= TP_{0s} = 9 bar for TP_s-curve II. Comparing the wheat model in Figure 10A with the oat model in Figure 8B, it is evident that TP_{0g} (the value of TP_g in darkness when WP_{intg}=0) is higher (15 instead of 9 bar), that the slopes of the TP_s-curves are higher at lower TP_g-values and that it is possible to close stomata for all values of TP_s. In the extrapolated oat model of Figure 8B, it is not possible to close stomata for TP_s-values between 0 and 6 bar.

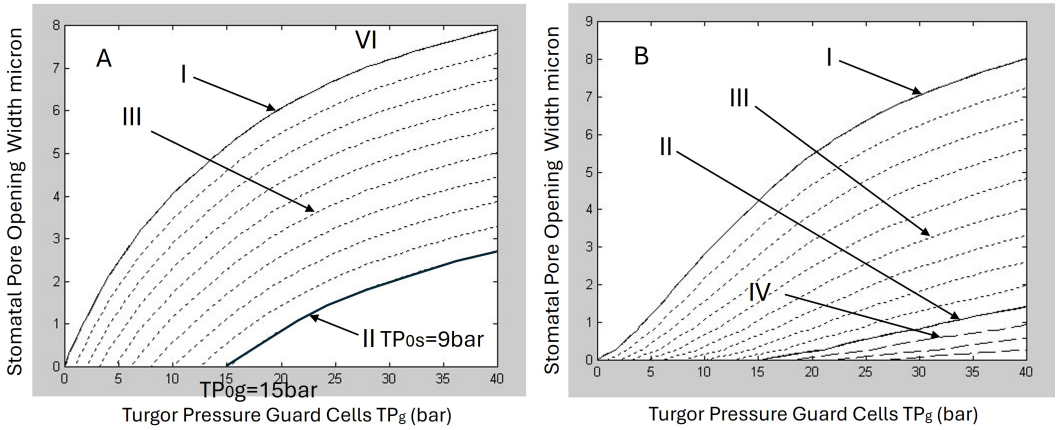

Figure 10: *TP_s-curves showing stomatal pore opening width for wheat as function of guard cells turgor TP_g. A: The TP_s-curves I and II are according to Franks and Farquhar (2007) and intermediate TP_s-curves (III) are interpolated TP_s-curves, separated by 1 bar. B: The TP-curves in Figure A after introduction of the same additional non-linearity as used for the oat model in Figure 9.*

Figure 10B shows the stomatal mechanics model in Figure 10A after adding the same non-linearity as in Figure 9. TP_s-curves (IV) for TP_s-values higher than TP_{0s} (9 bar) are inserted to show TP_s-values that can be obtained when hydro-active feedback to the subsidiary cells is used.

To obtain stomatal conductance in mm/s as output from the stomatal mechanics models, a parameter K_{oc} is used. In the case of oat, K_{oc} was chosen to 0.1 mm/s,micron^2. In the case of wheat, K_{oc} was selected to be 1 mm/s, micron. The values of K_{oc} were selected to obtain stomatal conductance values in the same range as in the simulations made by Cowan (1972).

A.6. Modelling of osmotic connection between guard- and subsidiary cells

To implement the influence of OSM_{refg} on OSM_{refs}, curve IV in Figure 8A, as proposed by Franks and Farquhar (2007) and by Durney et al. (2023), the relationship between cell volume of the guard cells (W_{0g} + dw_g, see Figure 5) and cell volume of the subsidiary cells (W_{0s} + dw_s) must be determined. If all the K^+ ions pumped into the guard cells originate from the subsidiary cells, the osmotic content increase (OSM_{refg}, see Figure 6) in the guard cells must be the same as the osmotic content reduction (OSM_{refs}) in the subsidiary cells and vice versa, which means that K_{gs}=-1 in Figure 6. To obtain the same light response as curve IV of Figure 8A, it is thus necessary to tune the relationship between the volumes W_{0g} and W_{0s} together with the relationship between dw_g and dw_s. Now, this

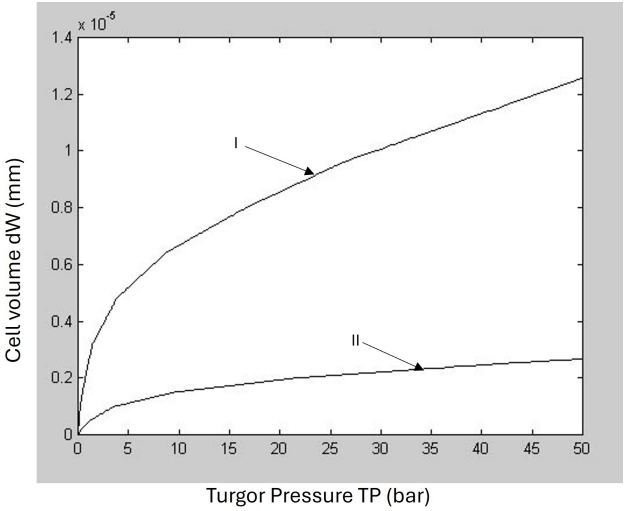

Figure 11: *Non-linearities used between turgor pressure TP and cell volume dw. I: Subsidiary cells, II: Guard cells. Observe that the cell volumes W_{0g} and W_{0s} at TP=0 bar are added in the cell models.*

task is quite difficult since dw is a nonlinear function of the turgor pressure and thus of the osmotic pressure. Figure 4 of Franks et al. (2001) shows results of measurements of the cell volume as function of the turgor pressure of the guard cells for Vicia faba. These results were used to design the non-linear relationships between TP and dw (defining NL_{dw} in Figure 5) for the guard- and subsidiary cells. Figure 11 shows the non-linearities used. With dw at 50 bar equal to W_0

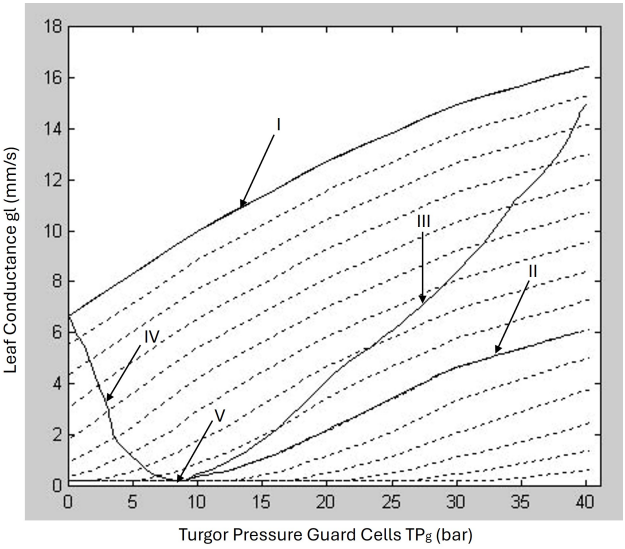

Figure 12: *Response to light with the subsidiary cells as osmotic provider for the guard cells (III) and without this concept (II). At the beginning of the simulations the cells are filled with osmotic substances, resulting in trajectory IV until TP_g=TP_s=9 bar at V. TP_s-curve I for TP_s=0 bar and II for 9 bar.*

(approximative from the results of Franks et al. (2001), different relations between W_{0s} and W_{0g} were tested. The larger W_{0s} is in relation to W_{0g}, the lower the derivative of curve IV in Figure 8A will be. In the presented simulations, both for oat and wheat, W_{0s} was set to be 5 times larger than W_{0g}.

Figure 12 shows simulation results using the oat stomatal mechanics model from Figure 9. In these simulations ip=0 mm/s and therefore no feedback system is active. At trajectory point V a light ramp is applied, giving a continuously increasing osmotic pressure in the guard cells, generating an increase of TP_g from 9 to 40 bar. Curve III is then obtained with K_{gs}=-1 while curve II is obtained without osmotic connection (K_{gs}=0). In both cases $W_{0s} = 5 \cdot W_{0g}$ and the non-linearities of Figure 11 were used. Because of non-linear effects, curve III will bend upwards at higher values of TP_g and will therefore deviate from curve IV in Figure 8A. To reduce the derivative of curve III, W_{0s} must be even larger in relation to W_{0g} or K_{gs} must be increased in the interval [-1, 0]. Increasing K_{gs} means that some of the osmotic substance entering the guard cells must originate from other sources than the subsidiary cells.

B. Model parameters

```
Rg = 1.0*10^10 bar*s/m;
Rs = 2.5*10^9 bar*s/m
Re = 1.2*10^9 bar*s/m;
Rm = 5*10^7 bar*s/m
Cg and Cs nonlinear, see Figure 11
Ce = 1.0*10^(-7) m/bar;
Cm = 1.5*10^(-6) m/bar
WOg = 2.44*10^(-6) mm;
WOs = 12.2*10^(-6) mm
Sg = s1;
Ss = s1;
Se = s2;
Sm = s2;
Kes = 0;
NLis: Limits of Is =+/-0.6*10^(-6) mm/s
NLig: No limits
```

Listing 1: Cell Module Parameters

```
Tlightpr = 13 min;
Tactg = 2.7 min;
Tacts = 2.7 min;
dttranspg = 1.3 min;
dttransps = 1.3 min;
dttranspe = 1.3 min;
Kgs = -1
Ke = -0.9
OSMtpOs ·2 · 10^-6 = 1.68*10^(-4) bar*mm
OSMtpOe = 9 bar
OSMtpOm = 9 bar
Oat:
OSMtpOg ·2 · 10^-6 = 3.52*10^(-5) bar*mm
Koc = 0.1 mm/s, micron^2
Wheat:
OSMtpOg ·2 · 10^-6 = 6.28*10^(-5) bar*mm
Koc = 1 mm/s, micron
```

Listing 2: Osmotic control module parameters

```
gc = 0.2 mm/s;
h = 10 mm/;
```

Listing 3: Evaporation module parameters

```
Rl = 1.0*e8 bar*s/m;
Rr = 1.5*e8 bar*s/m;
Re = 0.5*e8 bar*s/m;
```

Listing 4: Water flow module parameters

```
Figure 2:
OSMlight ·2 · 10^-6 = 6.48*10^(-5) bar*mm
Figure 2A:
Kg = 6.97;
ip = 0.78*10^(-4) mm/s;
Figure 2B:
Ks = -20.8;
ip = 0.73*10^(-4) mm/s;;
Figure 2C:
Kg = 3.56;
Ks = -11.7;
ip = 0.8*10^(-4) mm/s;
Figure 3:
OSMlight ·2 · 10^-6 = 1.35*10-4 bar*mm;
Figure 3A:
Kg = 11.48;
ip = 1.2*10^(-4) mm/s;
Figure 3B:
Ks = -25.4;
ip = 1.25*10^(-4) mm/s;
Figure 3C:
Kg = 8.1;
Ks = -14.3;
ip = 1.1*10^(-4) mm/s;
Figure 4A:
OSMlight ·2 · 10^-6 = 6.48*10^(-5) bar*mm;
Kg = 3.56;
Ks = -11.7;
Ip = from 0 to 0.55 *10^(-4) mm/s;
Figure 4B:
OSMlight ·2 · 10^-6 = 1.35*10-4 bar*mm
Kg = 8.1;
Ks = -14.3;
Ip = from 0 to 0.7 *10^(-4) mm/s;
Scaling of Kg and Ks:
K ·2 · 10^-6: will be in mm
```

Listing 5: Simulation specific parameters

References

Barrs, H. D. Cyclic variations in stomatal aperture, transpiration, and leaf water potential under constant environmental conditions. *Annual Review of Plant Biology*, 1971. 22:223–236. doi:10.1146/annurev.pp.22.060171.001255.

Bauer, H., Ache, P., Lautner, S., Fromm, J., Hartung, W., Al-Rasheid, K., Sonnewald, S., Sonnewald, U., Kneitz, S., Lachmann, N., Mendel, R., Bittner, F., Hetherington, A., and Hedrich, R. The Stomatal Response to Reduced Relative Humidity Requires Guard Cell-Autonomous ABA Synthesis. *Current Biology*, 2013. 23(1):53–57. doi:10.1016/j.cub.2012.11.022.

Brogårdh, T., Johnsson, A. B., and Klockare, R. Oscillatory Transpiration and Water Uptake of Avena Plants. V. Influences of the Water Potential of the Root Medium. *Physiologia Plantarum*, 1974. 32:258–267. doi:10.1111/J.1399-3054.1974.TB03132.X.

Brogårdh, T. and Johnsson, A. Oscillatory transpiration and water uptake of avena plants. *Physiologia Plantarum*, 1973. 28(2):341–345. doi:10.1111/j.1399-3054.1973.tb01198.x.

Buckley, T. N. The control of stomata by water balance. *New Phytologist*, 2005. 168(2):275–292. doi:10.1111/j.1469-8137.2005.01543.x.

Buckley, T. N. Stomatal responses to humidity: has the 'black box' finally been opened? *Plant, Cell & Environment*, 2016. 39(3):482–484. doi:10.1111/pce.12651.

Buckley, T. N. How do stomata respond to water status? *New Phytologist*, 2019. 224(1):21–36. doi:10.1111/nph.15899.

Buckley, T. N., Mott, K. A., and Farquhar, G. D. A hydromechanical and biochemical model of stomatal conductance. *Plant, Cell & Environment*, 2003. 26(10):1767–1785. doi:10.1046/j.1365-3040.2003.01094.x.

Büchsenschütz, K., Marten, I., Becker, D., Philippar, K., Ache, P., and Hedrich, R. Differential expression of K+ channels between guard cells and subsidiary cells within the maize stomatal complex. *Planta*, 2005. 222(6):968–976. doi:10.1007/s00425-005-0038-6.

Cinquin, O. and Demongeot, J. Roles of positive and negative feedback in biological systems. *Comptes Rendus Biologies*, 2002. 325(11):1085–1095. doi:10.1016/S1631-0691(02)01533-0.

Cong, X., Li, S., and Hu, D. Stomatal dynamics: a modeling study revisiting miscellaneous experimental phenomena. *Authorea*, 2022. doi:10.22541/au.166852604.48579873/v1.

Cong, X., Li, S., and Hu, D. Stomatal aperture dynamics coupling mechanically passive and ionically active mechanisms. *Plant, Cell & Environment*, 2024. 47(1):106–121. doi:10.1111/pce.14726.

Cotelle, V. and Leonhardt, N. Chapter Four - ABA signaling in guard cells. In M. Seo and A. Marion-Poll, editors, *Abscisic Acid in Plants*, volume 92 of *Advances in Botanical Research*, pages 115–170. Academic Press, 2019. doi:10.1016/bs.abr.2019.10.001.

Cowan, I. Oscillations in stomatal conductance and plant functioning associated with stomatal conductance: Observations and a model. *Planta*, 1972. 106(3):185–219. doi:10.1007/BF00388098.

Cui, Y., Zhao, Y., Lu, Y., Su, X., Chen, Y., Shen, Y., Lin, J., and Li, X. In vivo single-particle tracking of the aquaporin AtPIP2;1 in stomata reveals cell type-specific dynamics. *Plant Physiol.*, 2021. 185(4):1666:1681. doi:10.1093/plphys/kiab007.

Ding, L., Laurent, M. J., Milhiet, T., Aesaert, S., Van Lijsebettens, M., Pauwels, L., Nelissen, H., Inzé, D., and Chaumont, F. The maize aquaporin ZmPIP1;6 enhances stomatal opening and CO2- and ABA-induced stomatal closure. *Journal of Experimental Botany*, 2024. 76(10):2832–2845. doi:10.1093/jxb/erae500.

Durney, C. H., Wilson, M. J., McGregor, S., Armand, J., Smith, R. S., Gray, J. E., Morris, R. J., and Fleming, A. J. Grasses exploit geometry to achieve improved guard cell dynamics. *Current Biology*, 2023. 33(13):2814–2822.e4. doi:10.1016/j.cub.2023.05.051.

Farquhar, G. and Cowan, I. Oscillations in stomatal conductance: the influence of environmental gain. *Plant Physiol.*, 1974. 54(5):769–772. doi:10.1104/pp.54.5.769.

Franks, P., Buckley, T., Shope, J., and Mott, K. Guard cell volume and pressure measured concurrently by confocal microscopy and the cell pressure probe. *Plant Physiol.*, 2001. 125(4):1577–1584. doi:10.1104/pp.125.4.1577.

Franks, P., Cowan, I., and Farquhar, G. A study of stomatal mechanics using the cell pressure probe. *Plant, Cell & Environment*, 1998. 21(1):94–100. doi:10.1046/j.1365-3040.1998.00248.x.

Franks, P. and Farquhar, G. The mechanical diversity of stomata and its significance in gas-exchange control. *Plant Physiology*, 2007. 143(1):78–87. doi:10.1104/pp.106.089367.

Franks, P. J. Stomatal control and hydraulic conductance, with special reference to tall trees. *Tree Physiology*, 2004. 24(8):865–878. doi:10.1093/treephys/24.8.865.

Gumowski, I. Analysis of oscillatory plant transpiration. *Journal of Interdisciplinary Cycle Research*, 1981. 12(4):273–291. doi:10.1080/09291018109359752.

Haefner, J. W., Buckley, T. N., and Mott, K. A. A spatially explicit model of patchy stomatal responses to humidity. *Plant, Cell & Env.*, 1997. 20(9):1087–1097. doi:10.1046/j.1365-3040.1997.d01-137.x.

Hopmans, P. *Rhythms in stomatal opening of bean leaves*. PhD Thesis, Wageningen University & Research, Netherlands, 1971. doi:10.18174/191967.

Jasechko, S., Sharp, Z. D., Gibson, J. J., Birks, S. J., Yi, Y., and Fawcett, P. J. Terrestrial water fluxes dominated by transpiration. *Nature*, 2013. 496:347–350. doi:10.1038/nature11983.

Johnsson, A. Oscillations in plant transpiration. In S. Mancuso and S. Shabala, editors, *Rhythms in Plants: Dynamic Responses in a Dynamic Environment*, pages 157–188. Springer, Cham, 2015. doi:10.1007/978-3-319-20517-5_7.

Kuromori, T., Seo, M., and Shinozaki, K. Aba transport and plant water stress responses. *Trends in Plant Science*, 2018. 23(6):513–522. doi:10.1016/j.tplants.2018.04.001.

Liu, L., Ashraf, M., T., M., and M., F. Stomatal closure in maize is mediated by subsidiary cells and the PAN2 receptor. *New Phytol.*, 2024. 241(3):1130–1143. doi:10.1111/nph.19379.

Majore, I., Wilhelm, B., and Marten, I. Identification of K(+) channels in the plasma membrane of maize subsidiary cells. *Plant Cell Physiol.*, 2002. 43(8):855–852. doi:10.1093/pcp/pcf104.

McAdam, S., Sussmilch, F., and Brodribb, T. Stomatal responses to vapour pressure deficit are regulated by high speed gene expression in angiosperms. *Plant, Cell & Environment*, 2016. 39(3):485–491. doi:10.1111/pce.12633.

McAdam, S. A. M. and Brodribb, T. J. Mesophyll cells are the main site of abscisic acid biosynthesis in water-stressed leaves. *Plant Physiology*, 2018. 177(3):911–917. doi:10.1104/pp.17.01829.

Mumm, P., Wolf, T., Fromm, J., Roelfsema, M., and Marten, I. Cell type-specific regulation of ion channels within the maize stomatal complex. *Plant Cell Physiol.*, 2011. 52(8):1365–1375. doi:10.1093/pcp/pcr082.

Nieves-Cordones, M., Azeem, F., Long, Y., Boeglin, M., Duby, G., Mouline, K., Hosy, E., Vavasseur, A., Chérel, I., Simonneau, T., Gaymard, F., Leung, J., Gaillard, I., Thibaud, J.-B., Véry, A.-A., Boudaoud, A., and Sentenac, H. Non-autonomous stomatal control by pavement cell turgor via the K+ channel subunit AtKC1. *Plant Cell*, 2022. 34(5):2019–2037. doi:10.1093/plcell/koac038.

Prytz, G., Futsaether, C. M., and Johnsson, A. Thermography studies of the spatial and temporal variability in stomatal conductance of avena leaves during stable and oscillatory transpiration. *New Phytologist*, 2003. 158(2):249–258. doi:10.1046/j.1469-8137.2003.00741.x.

Raschke, K. and Fellows, M. Stomatal movement in zea mays: Shuttle of potassium and chloride between guard cells and subsidiary cells. *Planta*, 1971. 101(4):296–316. doi:10.1007/BF00398116.

Smolen, P., Baxter, D. A., and Byrne, J. H. Modeling circadian oscillations with interlocking positive and negative feedback loops. *Journal of Neuroscience*, 2001. 21(17):6644–6656. doi:10.1523/JNEUROSCI.21-17-06644.2001.

Tsai, T. Y.-C., Choi, Y. S., Ma, W., Pomerening, J. R., Tang, C., and Ferrell Jr, J. E. Robust, tunable biological oscillations from interlinked positive and negative feedback loops. *Science*, 2008. 321(5885):126–129. doi:10.1126/science.1156951.

Wang, G. X., Zhang, J., Liao, J.-X., and Wang, J.-L. Hydropassive evidence and effective factors in stomatal oscillations of glycyrrhiza inflata under desert conditions. *Plant Science*, 2001. 160(5):1007–1013. doi:10.1016/S0168-9452(01)00344-2.

Wolf, T., Heidelmann, T., and Marten, I. ABA Regulation of K+ -Permeable Channels in Maize Subsidiary Cells. *Plant and Cell Physiology*, 2006. 47(10):1372–1380. doi:10.1093/pcp/pcl007.

Zhang, L., Li, D., Yao, Y., and Zhang, S. H2O2, Ca2+, and K+ in subsidiary cells of maize leaves are involved in regulatory signaling of stomatal movement. *Plant Physiology and Biochemistry*, 2020. 152:243–251. doi:10.1016/j.plaphy.2020.04.045.